

Electronic Supplementary Information

for

Supramolecular intermediates in thermo-mechanochemical direct amidations

Tomislav Stolar,^{*a†} Jasna Alić,^a Gregor Talajić,^b Nikola Cindro,^b Mirta Rubčić,^b Krešimir Molčanov,^a Krunoslav Užarević,^{*a} José G. Hernández^{*c}

^a Ruđer Bošković Institute, Bijenička c. 54, 10000 Zagreb, Croatia.

^b Department of Chemistry, Faculty of Science, University of Zagreb, Horvatovac 102a, 10000 Zagreb, Croatia.

^c Grupo Ciencia de los Materiales, Instituto de Química, Facultad de Ciencias Exactas y Naturales, Universidad de Antioquia, Calle 70 No 52-21, 050010 Medellín, Colombia.

[†] Current address: Federal Institute for Materials Research and Testing (BAM), 12489 Berlin, Germany.

E-mail: tomislav.stolar@gmail.com; krunoslav.uzarevic@irb.hr; joseg.hernandez@udea.edu.co

Contents

General	2
Crystallography for compounds 3, 4, and 8	2
Results and analysis	7
Green chemistry metrics	19
Oven heating.....	20
Synthetic procedures	21
References.....	27

General

Benzoic acid (**1**) was purchased from TCI, *p*-toluidine (**2**) and cyclohexanamine (**10**) from Sigma-Aldrich, 4-chlorobenzoic (**6**) acid from Acros, and 4-(2-aminoethyl)morpholine (**7**) from Acros. Ball milling experiments were conducted with IST 500 vibratory ball mill using 12 mL volume stainless steel jars with two 7 mm balls of the same material. LAG experiments were conducted with 100 mg of *N*-(*p*-tolyl)-benzamide and 0.25 μL of H_2O as a liquid additive (η ratio of 0.2 $\mu\text{L}/\text{mg}$). PXRD patterns were collected on a PanAlytical Aeris diffractometer (Cu $\text{K}\alpha$ radiation and Ni filter) in Bragg-Brentano geometry using zero background sample holder. *In situ* monitoring of grinding benzoic acid and *p*-toluidine was performed at the P02.1 beamline at PETRA III, DESY (Hamburg, Germany). For *in situ* monitoring, ball milling was conducted with IST-636 mixer mill (InSolido Technologies, Croatia, Zagreb). We used 200 mg of the equimolar reaction mixture, 14 mL poly(methyl methacrylate) (PMMA) jars and two 7 mm stainless steel balls. The X-ray beam ($\lambda = 0.20741 \text{ \AA}$) was set to pass through the bottom of the PMMA reaction vessel. Exposure time was set to 10 s. Diffraction data were collected on a Perkin Elmer XRD1621 flat-panel detector positioned 1595 mm from the sample, which consisted of an amorphous Si sensor equipped with a CsI scintillator (pixel number: 2048 x 2048, pixel size: 200x200 μm^2). To obtain the classic one-dimensional PXRD pattern, the two-dimensional diffraction images were integrated with the DAWN Science package. NMR spectra were recorded on Bruker Ascend 400 MHz instrument at 298 K in $\text{DMSO-}d_6$ and were calibrated using residual non-deuterated solvent as an internal reference (DMSO: ^1H NMR $\delta = 2.50$ ppm, ^{13}C NMR $\delta = 39.52$ ppm). The following abbreviations were used to explain NMR peak multiplicities: s = singlet, d = doublet, m = multiplet, br = broad. Differential scanning calorimetry (DSC) analysis was performed with a TA DSC 25 calorimeter using standard aluminum pans. Between 1.0 mg and 2.0 mg of sample were used. All experiments were conducted in a dynamic nitrogen atmosphere with a flow rate of 50 $\text{cm}^3 \text{ min}^{-1}$ and with heating rate of 10 K min^{-1} .

Crystallography for compounds **3**, **4**, and **8**

Single crystals of **3** were grown by recrystallisation in H_2O . Single crystals of **4** were grown by melt cooling directly in the jar after milling **1** and **2** for 3 h at 190 $^\circ\text{C}$. Single crystals of **8** were grown by recrystallisation in THF. Single crystal measurements were performed on XtaLAB Synergy, Dualflex, HyPix (micro-focus sealed X-ray tube). Program package CrysAlis PRO¹ was used for data reduction and numerical absorption correction. The structures were solved using SHELXS97 and SHELXT and refined with SHELXL-2017.² In case of **3**, since *p*-toluidine lies in the centre of inversion, half of the amino group (N2) and half of the methyl group (C18) were refined with occupancy of 50 %. Models were refined using the full-matrix least squares

refinement; all non-hydrogen atoms were refined anisotropically. Hydrogen atoms were located in a difference Fourier map and refined as a mixture of free restrained and riding entities. Molecular geometry calculations were performed by PLATON.³ The crystal structures solved in this work were deposited in Cambridge Crystallographic Data Centre (CCDC) with the following deposition numbers: 2287226 (compound **3**), 2287225 (compound **4**), and 2285230 (compound **8**). The data can be obtained free of charge from the CCDC via www.ccdc.cam.ac.uk/data_request/cif.

Table S1. Crystallographic, data collection and refinement data for single crystal X-ray diffraction (compound **3**).

Compound	3
Empirical formula	C ₄₉ H ₅₁ N ₃ O ₈
Formula wt. / g mol ⁻¹	809.93
Colour	colourless
Crystal dimensions / mm	0.30 x 0.15 x 0.05
Space group	<i>P</i> 2 ₁ / <i>n</i>
<i>a</i> / Å	16.3249(3)
<i>b</i> / Å	6.11590(10)
<i>c</i> / Å	21.4268(3)
<i>α</i> / °	90
<i>β</i> / °	91.6370(10)
<i>γ</i> / °	90
<i>Z</i>	2
<i>V</i> / Å ³	2138.41(6)
<i>D</i> _{calc} / g cm ⁻³	1.258
<i>λ</i> / Å	1.54184 (CuKα)
<i>μ</i> / mm ⁻¹	0.691
<i>θ</i> range / °	3.358 – 79.876
<i>T</i> / K	100(2)
Diffraction type	XtaLAB Synergy
	-20 < <i>h</i> < 20;
Range of <i>h</i> , <i>k</i> , <i>l</i>	-6 < <i>k</i> < 7;
	-27 < <i>l</i> < 26

Reflections collected	16943
Independent reflections	4564
Observed reflections ($I \geq 2\sigma$)	4081
Absorption correction	Multi-scan
T_{\min} , T_{\max}	0.569 ; 1.0000
R_{int}	0.0529
R (F)	0.052
R_w (F^2)	0.1495
Goodness of fit	1.081
H atom treatment	Mixed
No. of parameters	281
No. of restraints	2
$\Delta\rho_{\max}$, $\Delta\rho_{\min}$ ($e\text{\AA}^{-3}$)	0.338 ; -0.297

Table S2. Crystallographic, data collection and refinement data for single crystal X-ray diffraction (compound **4**).

Compound	4
Empirical formula	$C_{21} H_{21} N O_4$
Formula wt. / g mol ⁻¹	351.39
Colour	colourless
Crystal dimensions / mm	0.28 x 0.16 x 0.04
Space group	$P2_1/n$
a / Å	11.5963(2)
b / Å	6.31630(10)
c / Å	25.5385(5)
α / °	90
β / °	92.362(2)
γ / °	90
Z	4
V / Å ³	1869.00(6)

$D_{\text{calc}} / \text{g cm}^{-3}$	1.249
$\lambda / \text{\AA}$	1.54184 (CuK α)
μ / mm^{-1}	0.704
Θ range / $^{\circ}$	3.464 – 79.643
T / K	100(2)
Diffraction type	XtaLAB Synergy
	$-24 < h < 14$;
Range of h, k, l	$-7 < k < 7$;
	$-32 < l < 28$
Reflections collected	14783
Independent reflections	3980
Observed reflections ($I \geq 2\sigma$)	3520
Absorption correction	Multi-scan
$T_{\text{min}}, T_{\text{max}}$	0.48039 ; 1.0000
R_{int}	0.0664
$R (F)$	0.0564
$R_w (F^2)$	0.1602
Goodness of fit	0.938
H atom treatment	Mixed
No. of parameters	248
No. of restraints	0
$\Delta\rho_{\text{max}}, \Delta\rho_{\text{min}} (\text{e}\text{\AA}^{-3})$	0.349 ; -0.352

Table S3. Crystallographic, data collection and refinement data for single crystal X-ray diffraction (compound **8**).

Compound	8
Empirical formula	C ₁₃ H ₁₉ Cl N ₂ O ₃
Formula wt. / g mol ⁻¹	286.75
Colour	colourless
Crystal dimensions / mm	0.33 x 0.08 x 0.05

Space group	$P2_1/n$
$a / \text{\AA}$	19.8713(4)
$b / \text{\AA}$	6.40620(10)
$c / \text{\AA}$	24.5625(4)
$\alpha / ^\circ$	90
$\beta / ^\circ$	106.679(2)
$\gamma / ^\circ$	90
Z	8
$V / \text{\AA}^3$	2995.24(10)
$D_{\text{calc}} / \text{g cm}^{-3}$	1.272
$\lambda / \text{\AA}$	1.54184 (CuK α)
μ / mm^{-1}	2.318
Θ range / $^\circ$	2.6340 – 79.0440
T / K	298(2)
Diffractometer type	XtaLAB Synergy
	-23 < h < 23;
Range of h, k, l	-7 < k < 7;
	-29 < l < 29
Reflections collected	54789
Independent reflections	5461
Observed reflections ($I \geq 2\sigma$)	4972
Absorption correction	Multi-scan
$T_{\text{min}}, T_{\text{max}}$	0.57483; 1.0000
R_{int}	0.0382
$R (F)$	0.0504
$R_w (F^2)$	0.1444
Goodness of fit	1.055
H atom treatment	Constr
No. of parameters	340
No. of restraints	7
$\Delta\rho_{\text{max}}, \Delta\rho_{\text{min}} (\text{e}\text{\AA}^{-3})$	0.346; -0.346

Results and

analysis

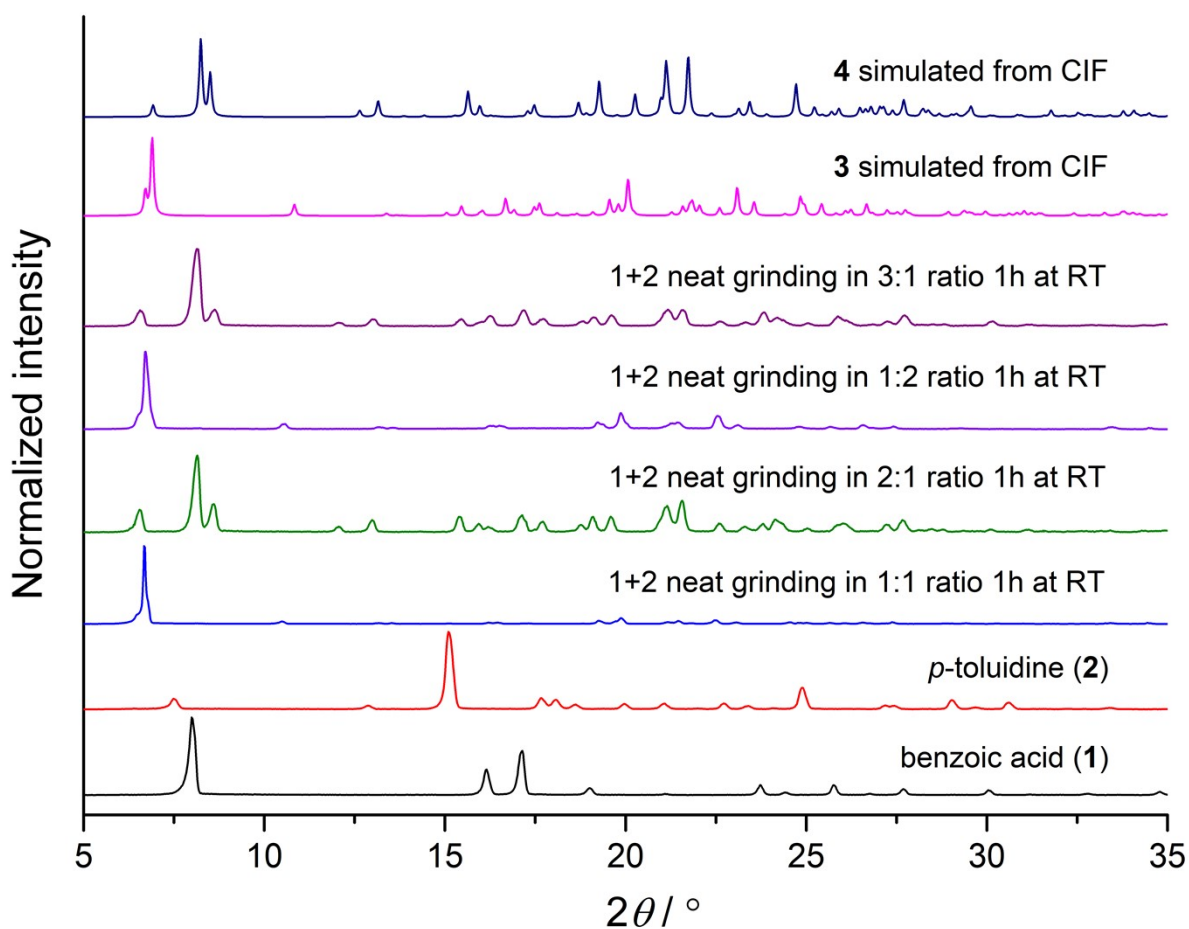


Figure S1. PXRD patterns for the system of benzoic acid and *p*-toluidine ($\lambda = 1.54 \text{ \AA}$). Patterns of **3** and **4** are simulated from CIFs (this work). Note that there is a slight mismatch between horizontal positions of Bragg reflections between experimental and simulated patterns of **3** and **4**. This is because single crystal X-ray diffraction measurements were collected at 100 K vs powder X-ray diffraction that was collected at room temperature.

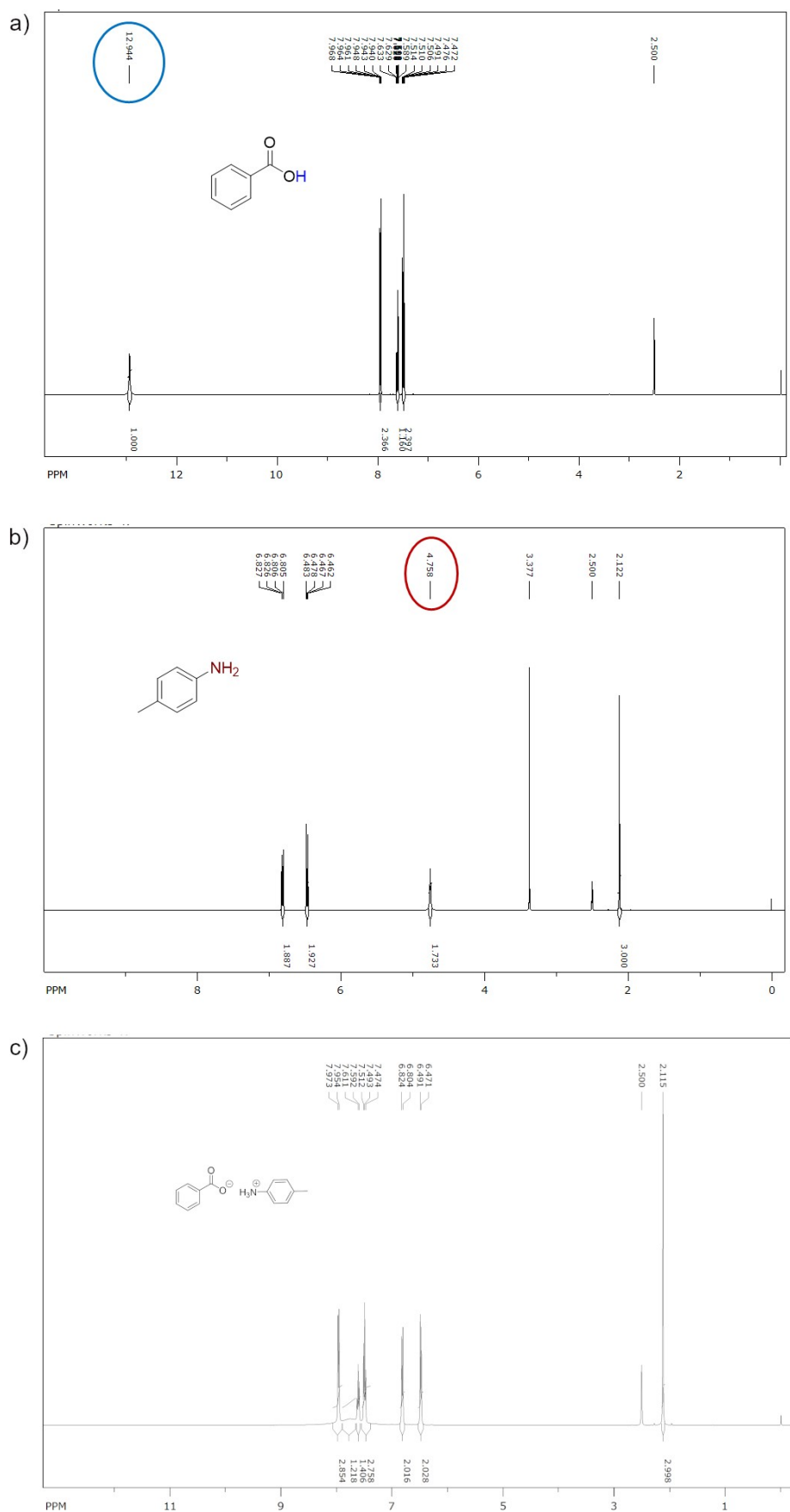


Figure S2. ^1H NMR spectra in $\text{DMSO}-d_6$ of: a) benzoic acid (**1**), b) *p*-toluidine (**2**), and c) a mixture of benzoic acid (**1**) and *p*-toluidine (**2**) neat grinded in 1:1 ratio for 1 h at room temperature (salt formation).

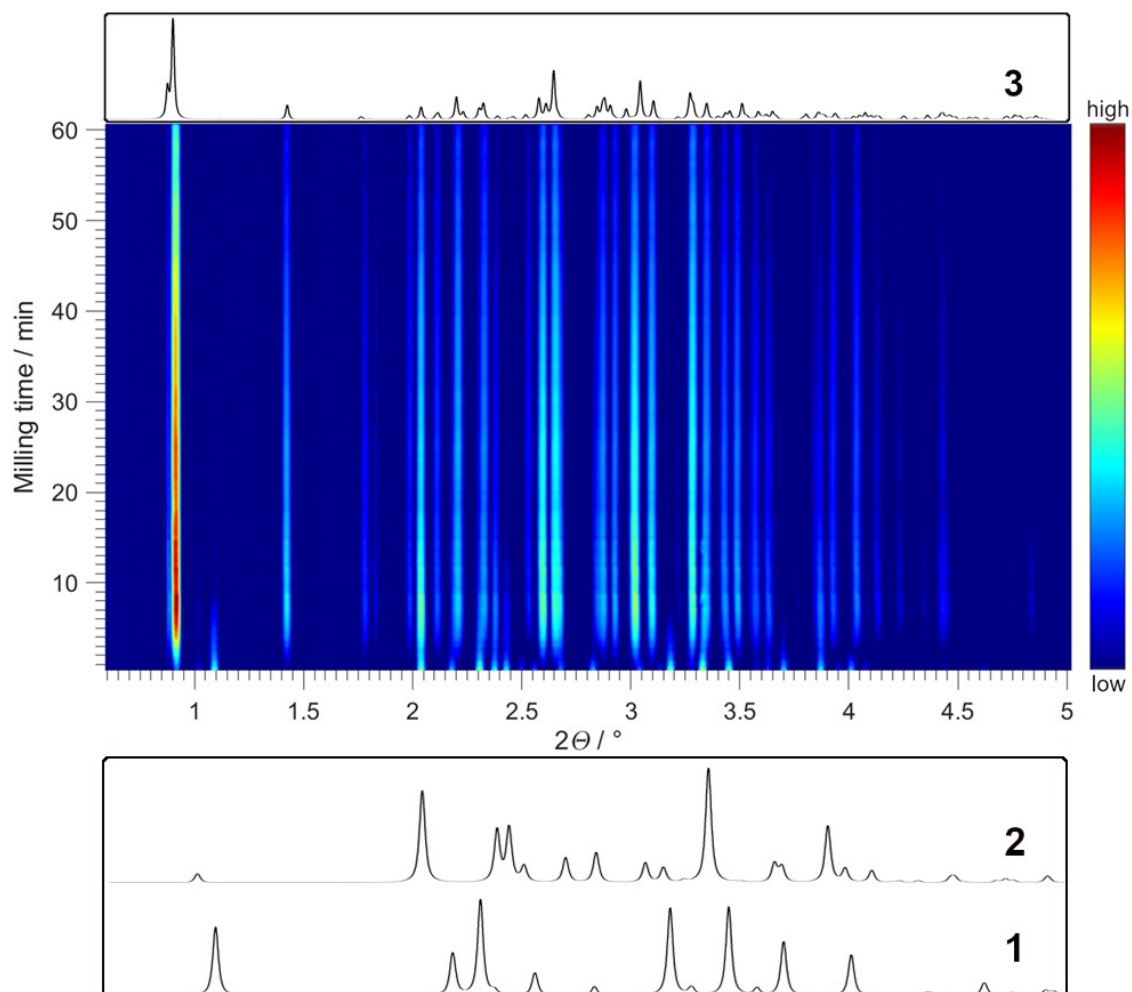


Figure S3. *In situ* monitoring by synchrotron PXRD ($\lambda = 0.207316 \text{ \AA}$) of grinding equimolar amount of benzoic acid (**1**) and *p*-toluidine (**2**) at room temperature. Simulated PXRD pattern of the corresponding ammonium carboxylate salt (**3**) is given in a box at the top, whereas **1** and **2** are at the bottom.

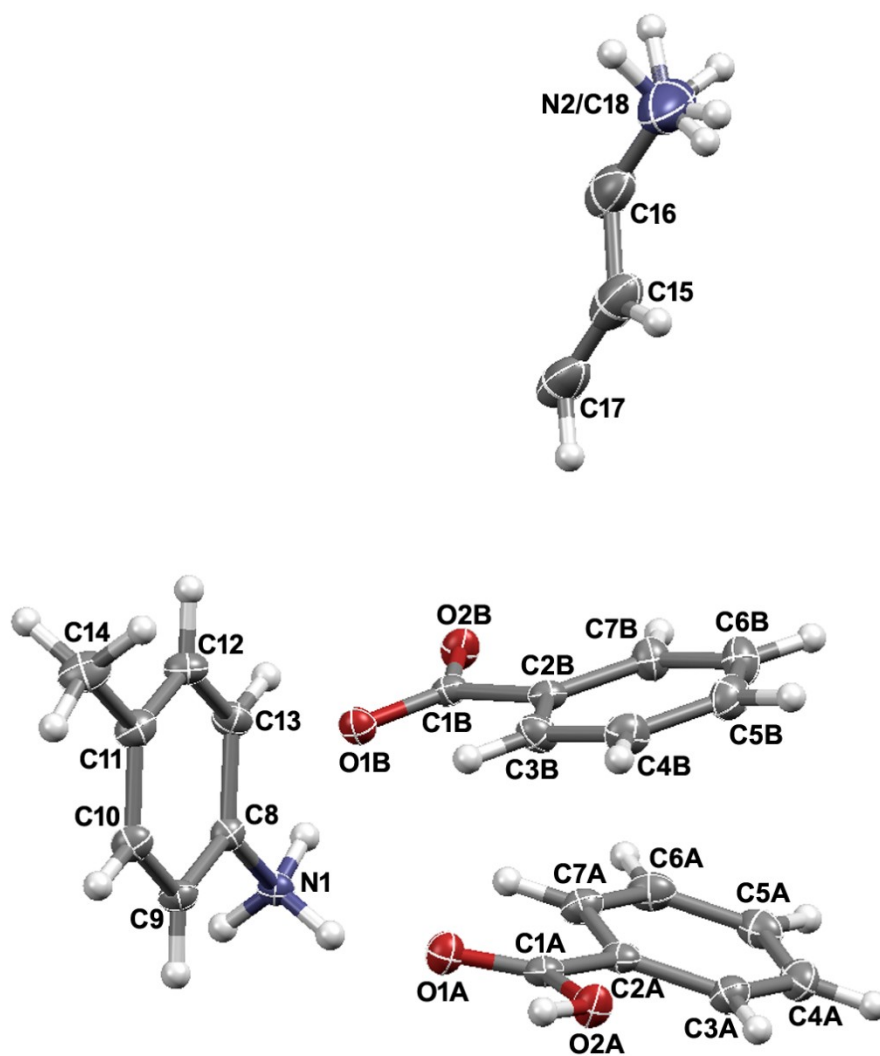


Figure S4. The asymmetric unit of **3** with the atom labeling scheme. Crystallographic inversion center coincides with the centroid of the ring defined by C16, C15, C17 atoms. Ellipsoids are drawn at 50% probability level, while hydrogen atoms are shown as small spheres of arbitrary radii.

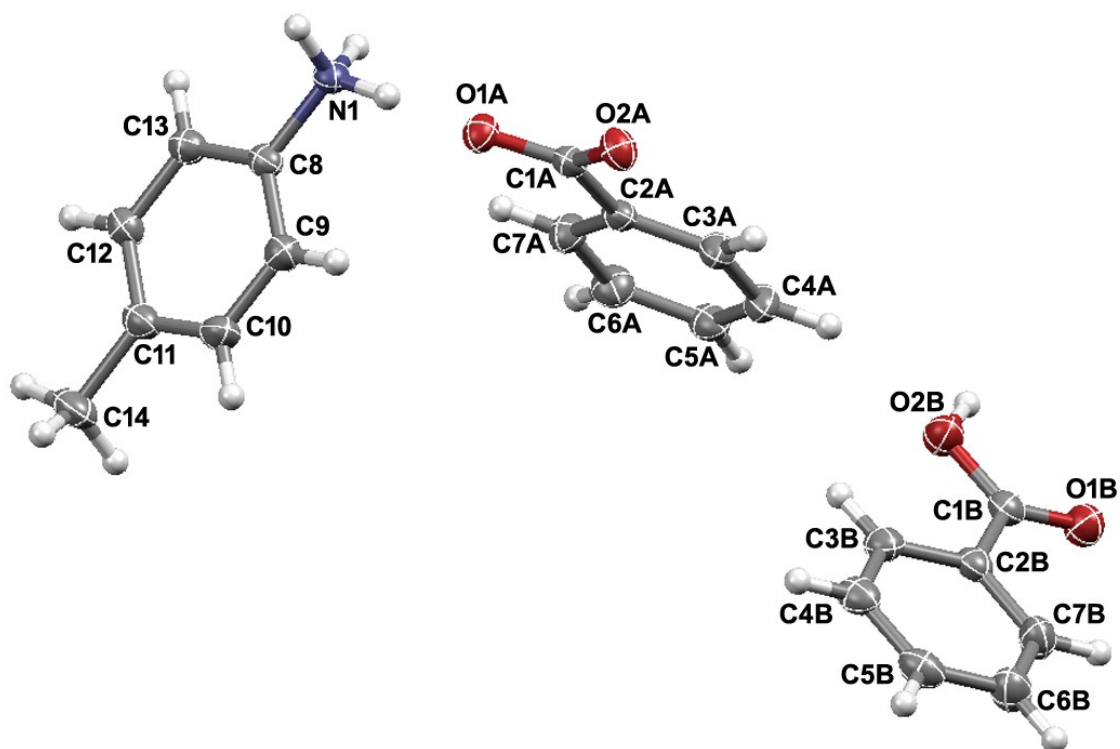


Figure S5. The asymmetric unit of **4** with the atom labeling scheme. Ellipsoids are drawn at 50% probability level, whereas hydrogen atoms are shown as small spheres of arbitrary radii.

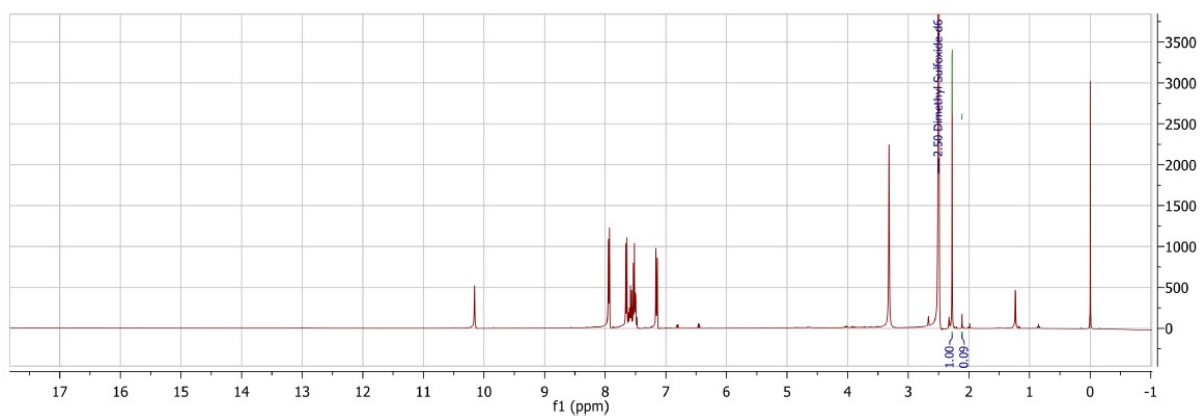


Figure S6. ^1H NMR spectra in $\text{DMSO-}d_6$ after milling **1** and **2** in 1:1 ratio for total 3 h at 190 $^\circ\text{C}$. The conversion was calculated as a ratio of signal corresponding to the methyl group in *p*-toluidine (**2**) (2.11 ppm) and in *N*-(*p*-tolyl)benzamide (**5**) (2.28 ppm).

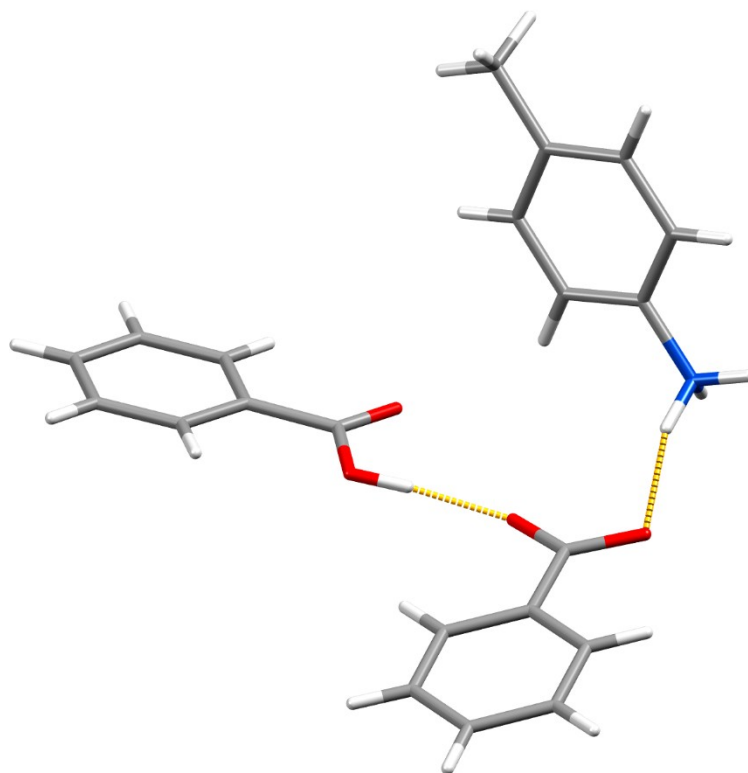


Figure S7. Fragment of the crystal structure of **4** showing hydrogen bonding interactions between protonated *p*-toluidine and one molecule of deprotonated benzoic acid which forms O-H \cdots O hydrogen bond to the second neutral molecule of benzoic acid.

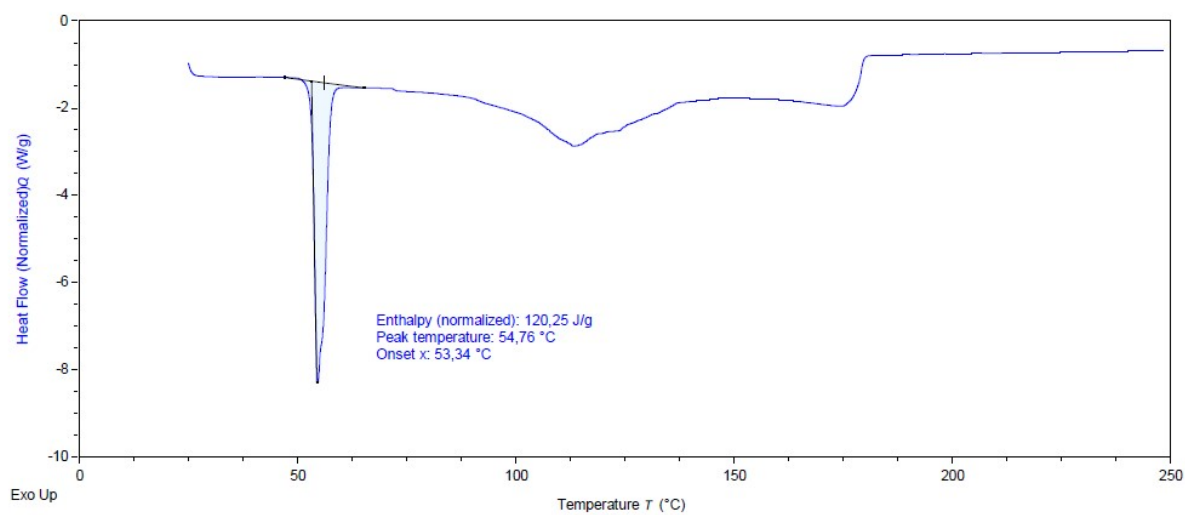


Figure S8. DSC trace of **3**. Peak temperature of melting is evident at 54.76 °C.

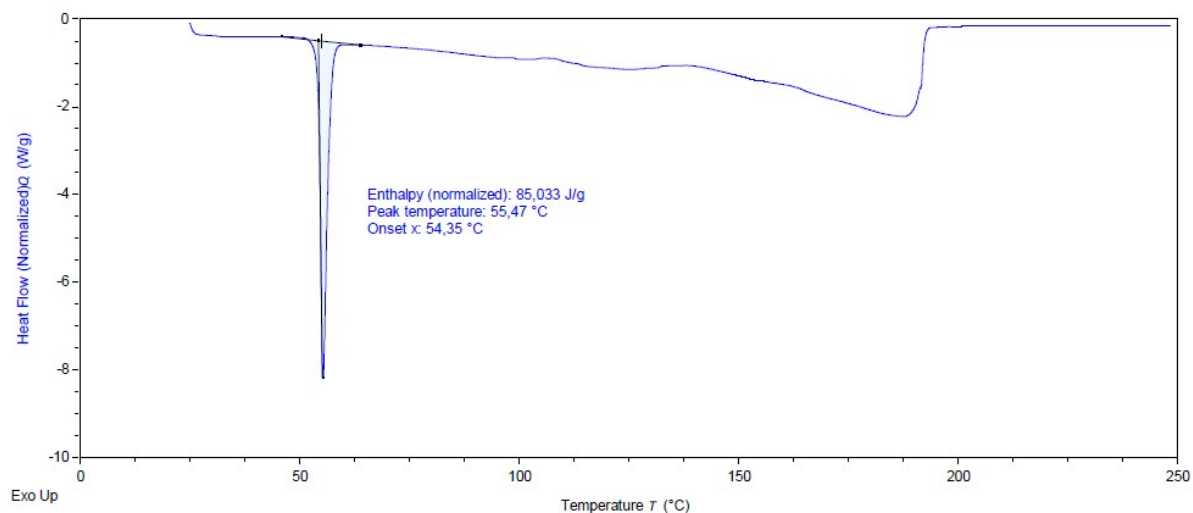


Figure S9. DSC trace of **4**. Peak temperature of melting is evident at 55.47 °C.

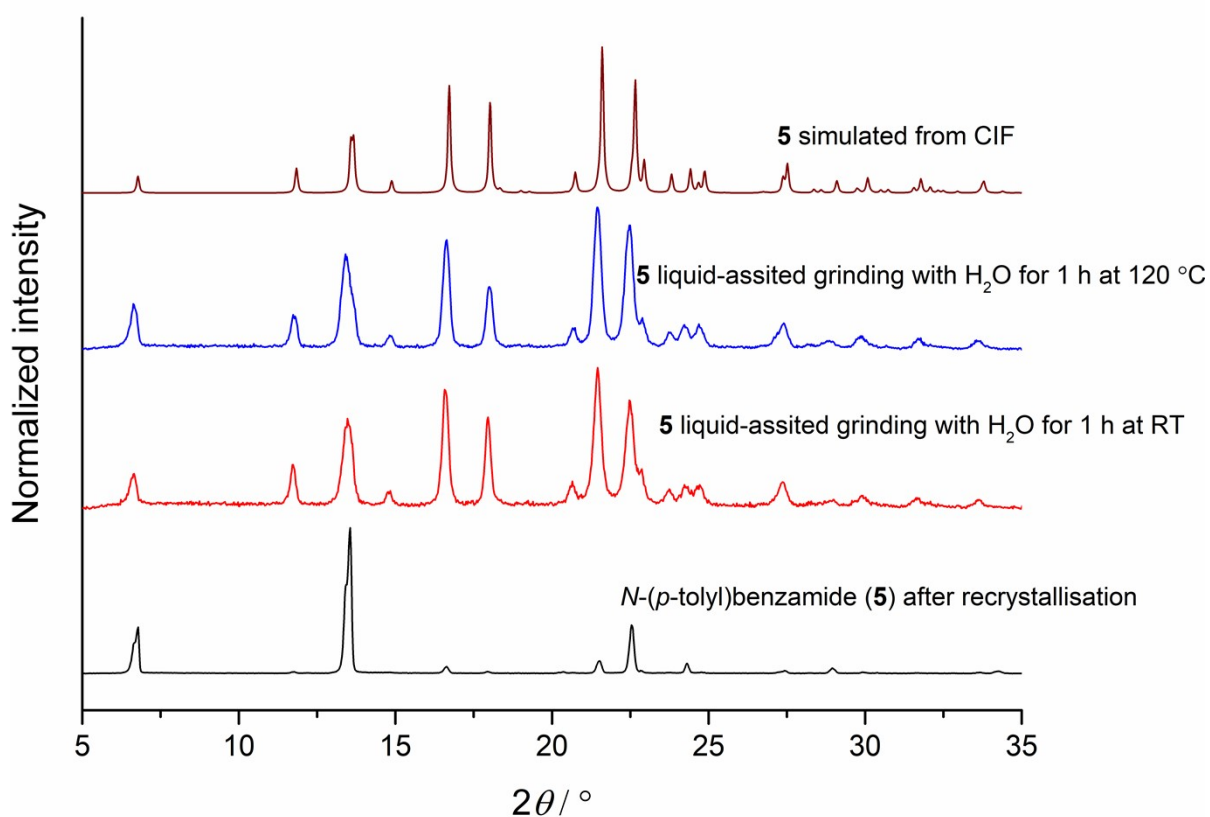


Figure S10. PXRD patterns of the reaction mixtures after liquid-assisted grinding **5** with H₂O at different temperatures and comparison with the starting material and simulated pattern of **5** from CIF ($\lambda = 1.54 \text{ \AA}$). CCDC code for simulated CIF of **5**: 674426.

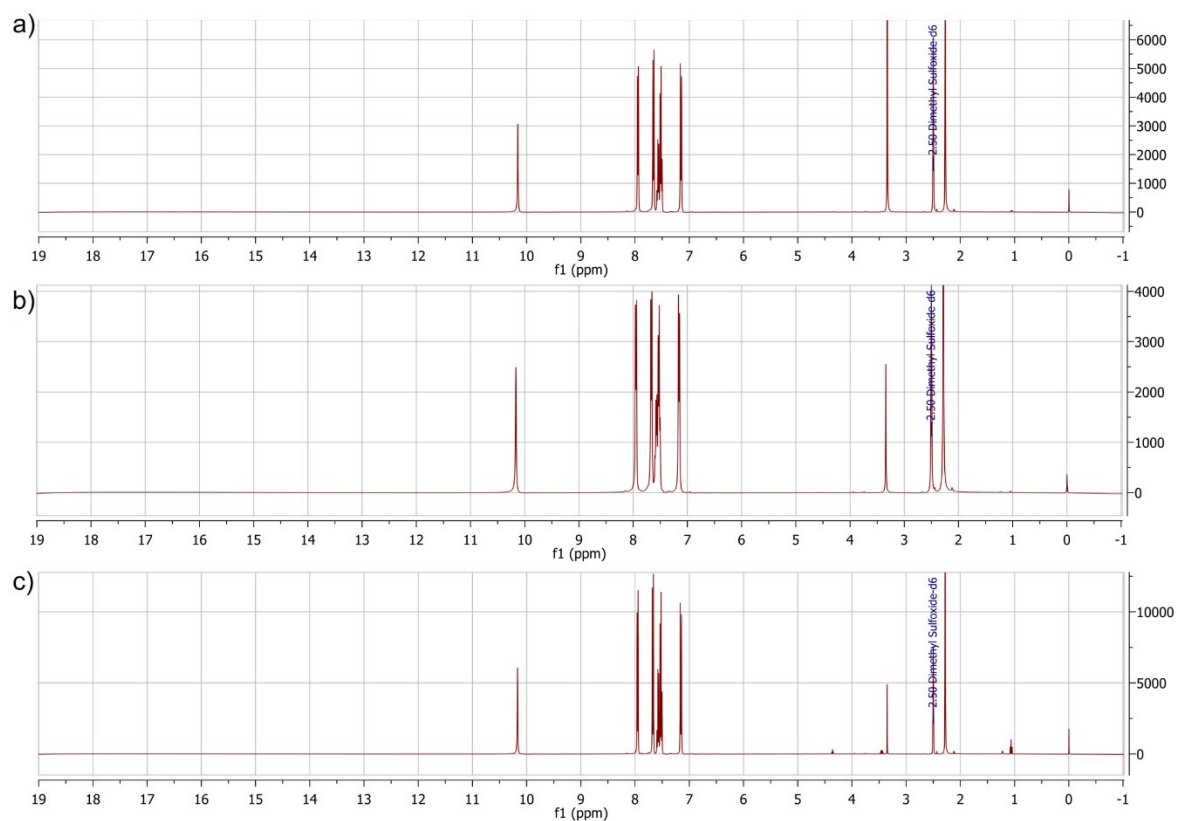


Figure S11. ^1H NMR spectra in $\text{DMSO-}d_6$ of: a) *N*-(*p*-tolyl)benzamide (**5**) liquid-assisted grinded with H_2O for 1 h at room temperature. b) *N*-(*p*-tolyl)benzamide (**5**) liquid-assisted grinded with H_2O for 1 h at 120°C . c) *N*-(*p*-tolyl)benzamide (**5**) that was used for liquid-assisted grinding reactions.

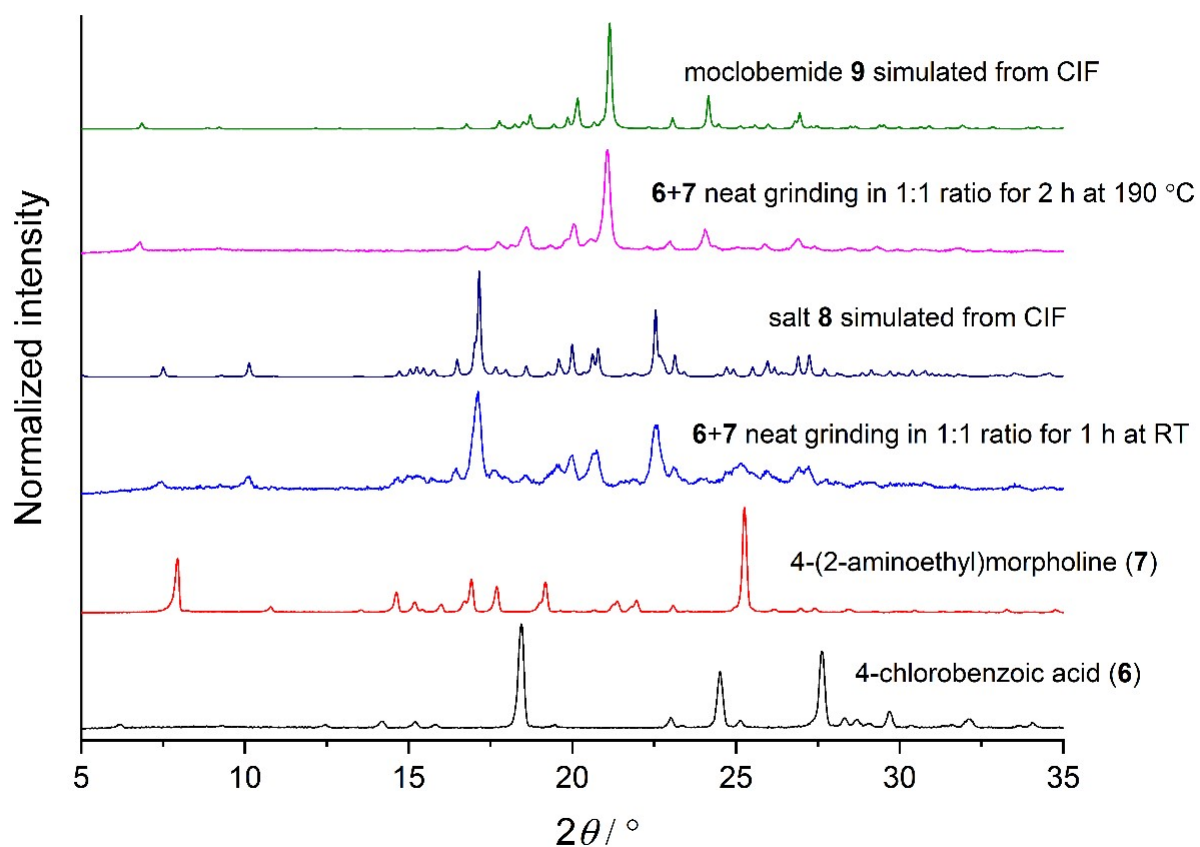


Figure S12. PXR D analysis of crude reaction mixtures after milling equimolar amounts of **6** and **7** at the room temperature and 190°C ($\lambda = 1.54 \text{ \AA}$). Phase pure **9** was obtained directly from the milling jar (CCDC code for simulated CIF of **9**: 1292693).

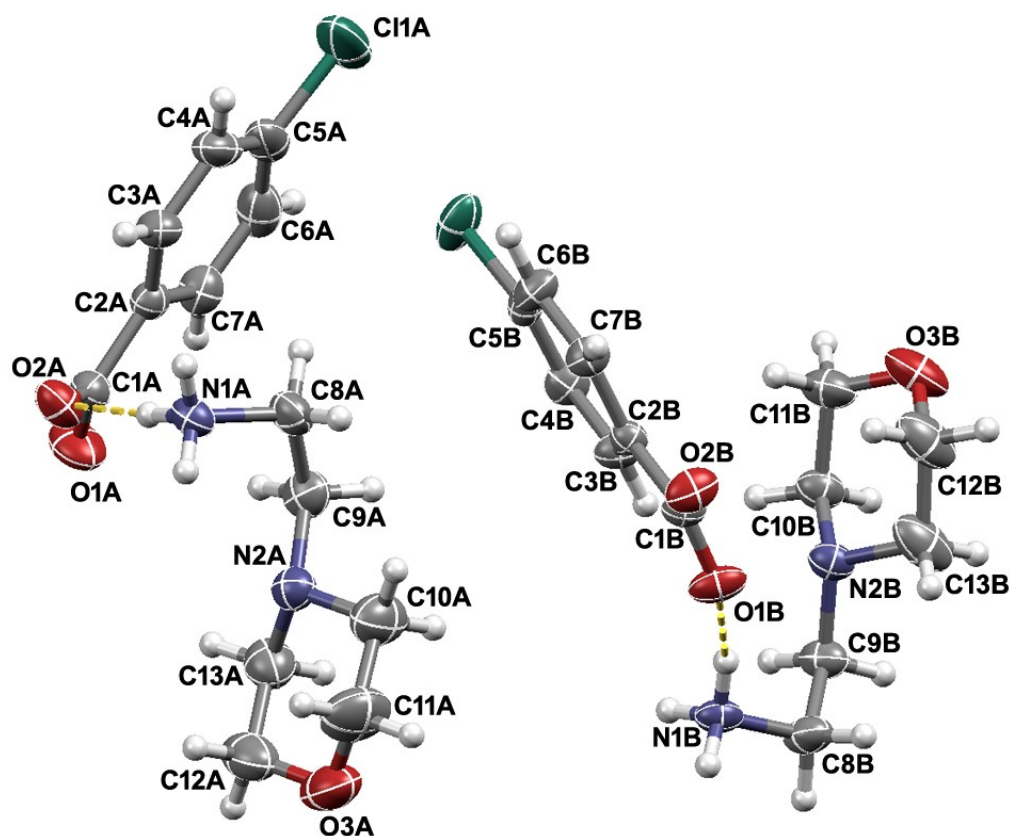


Figure S13. The asymmetric unit of **8** with the corresponding labeling scheme. The asymmetric unit embraces two anions of **6** and two cations of **7**. Ions of **6** and **7** labeled with A form chains A, whereas those labeled with B form chains B. Ellipsoids are drawn at 30% probability level, while hydrogen atoms are shown as small spheres of arbitrary radii. N–H···O hydrogen bonds are highlighted by yellow dashed lines.

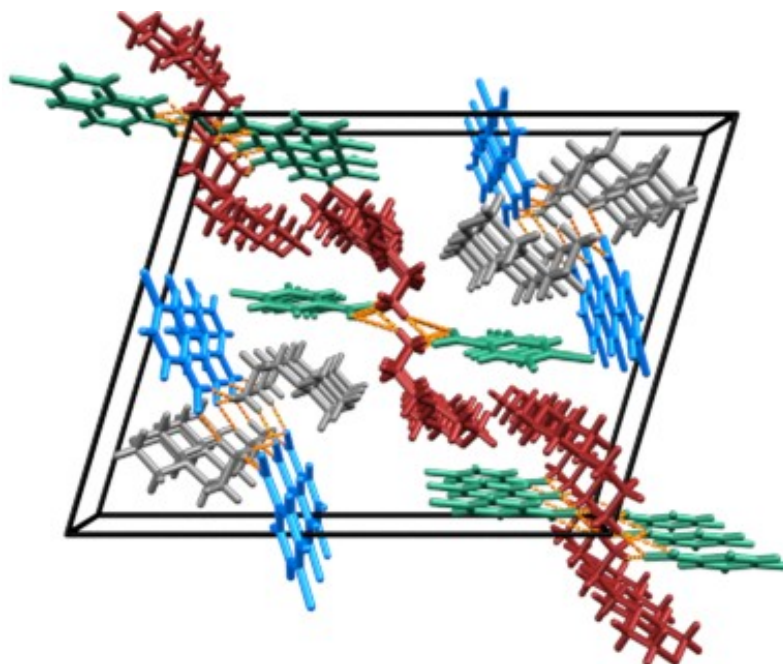


Figure S14. Crystal packing of **8** down the crystallographic *b*-axis. Chain A blue-gray; chain B green-red.

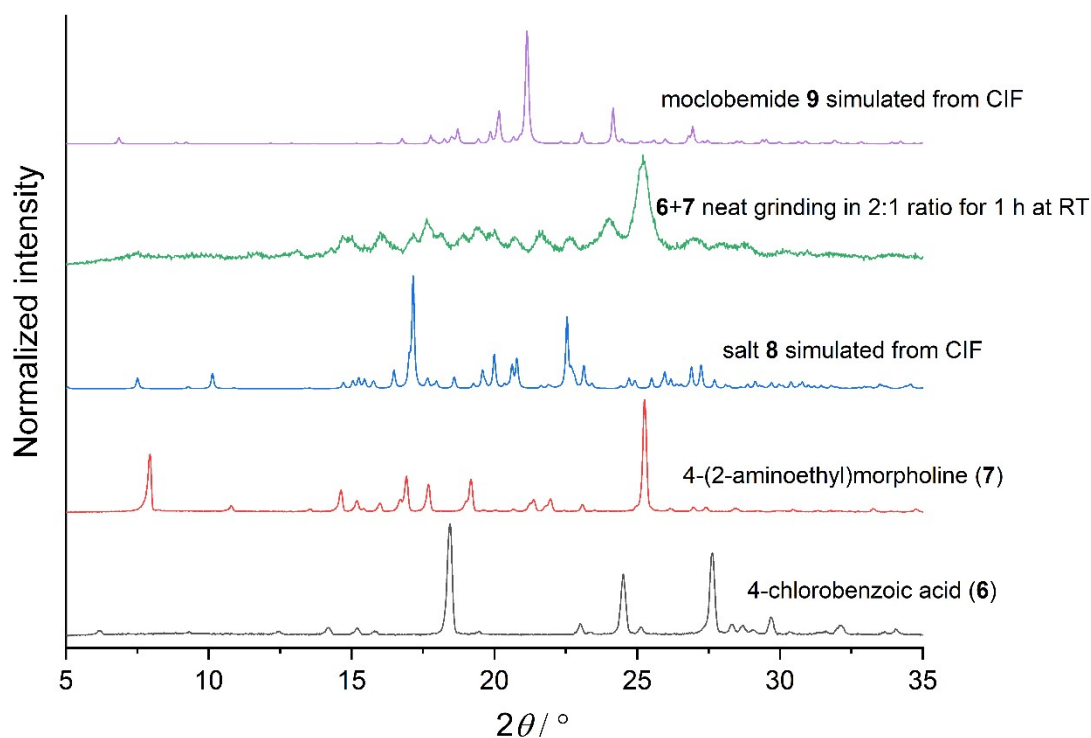


Figure S15. PXRD patterns of the reaction mixture after neat grinding **6** and **7** in 2:1 ratio for 1 h at RT (green) and comparison with the starting materials and simulated patterns of **8** (this work) and **9** ($\lambda = 1.54 \text{ \AA}$). CCDC code for simulated CIF of **9**: 1292693.

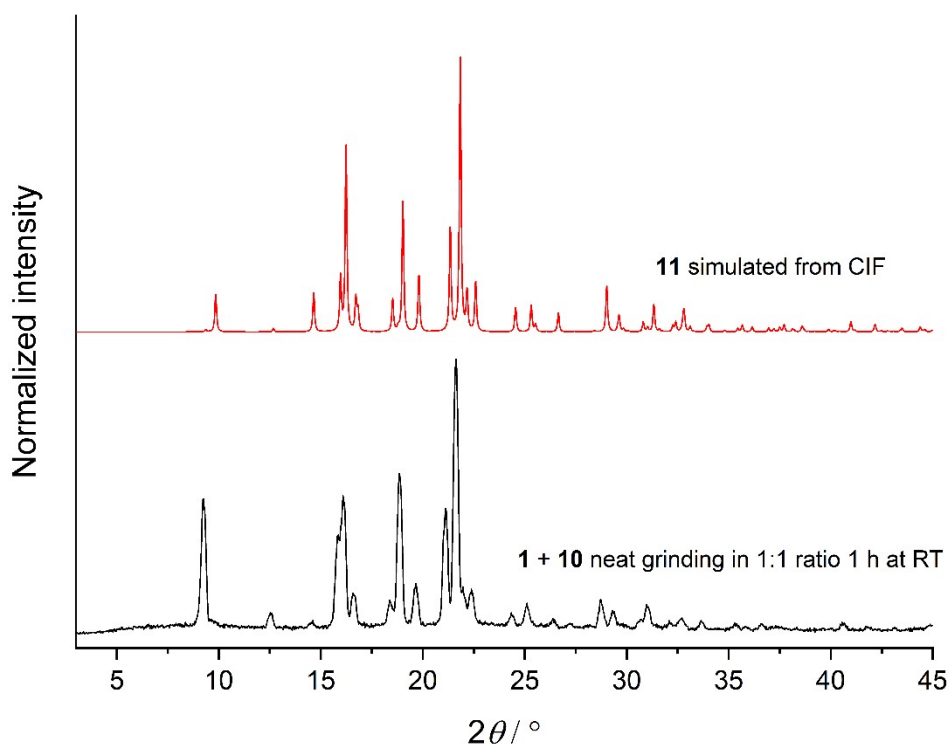


Figure S16. PXRD pattern of the reaction mixture after neat grinding benzoic acid (**1**) and cyclohexanamine (**10**) in 1:1 ratio for 1 h at room temperature and comparison to simulated PXRD pattern of their resulting ammonium carboxylate salt (**11**) ($\lambda = 1.54 \text{ \AA}$). CCDC code for simulated CIF of **11**: 797974.

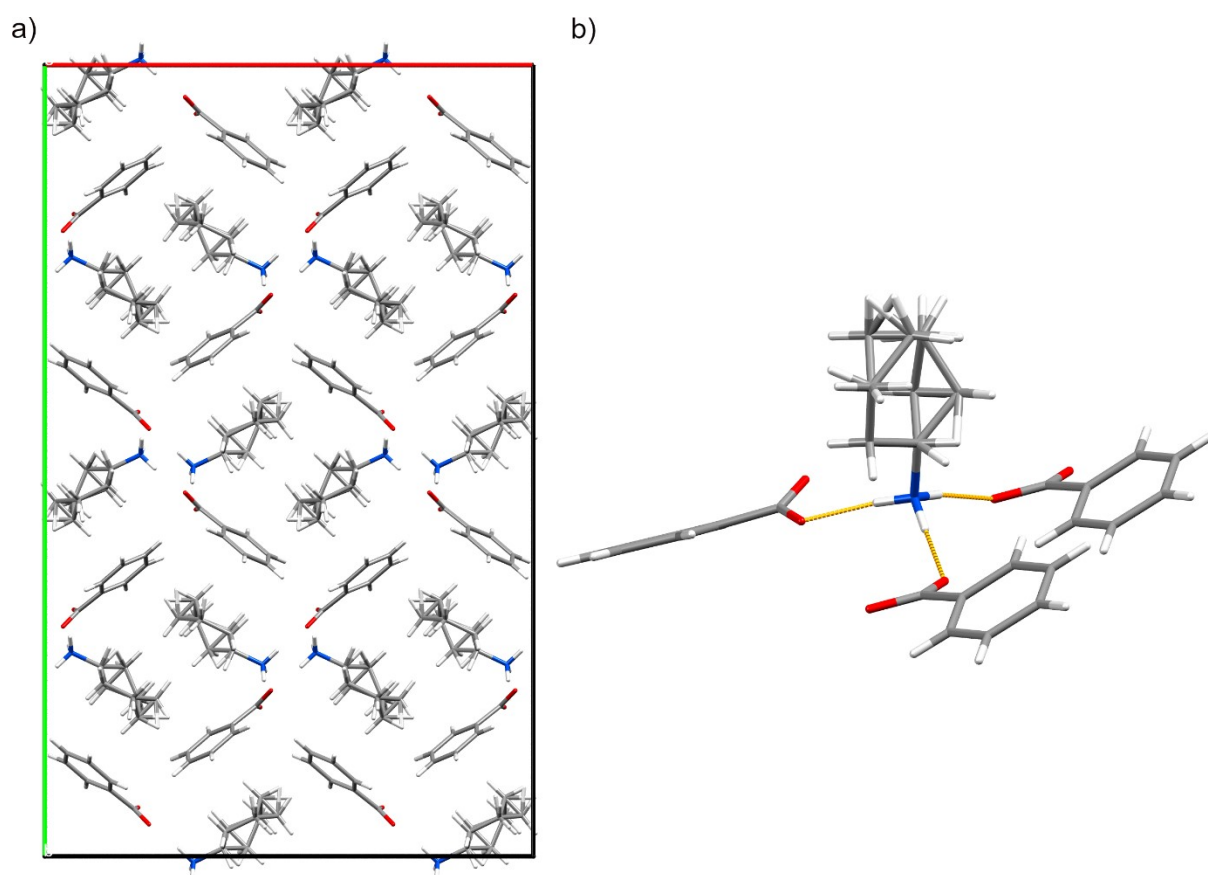


Figure S17. a) Unit cell of ammonium carboxylate salt of benzoic acid and cyclohexanamine (**11**). Note that cyclohexyl ring is disordered. b) Fragment of the crystal structure of **11** showing protonated cyclohexanamine molecule hydrogen bonding to three deprotonated molecules of benzoic acid. Note that cyclohexyl ring is disordered.

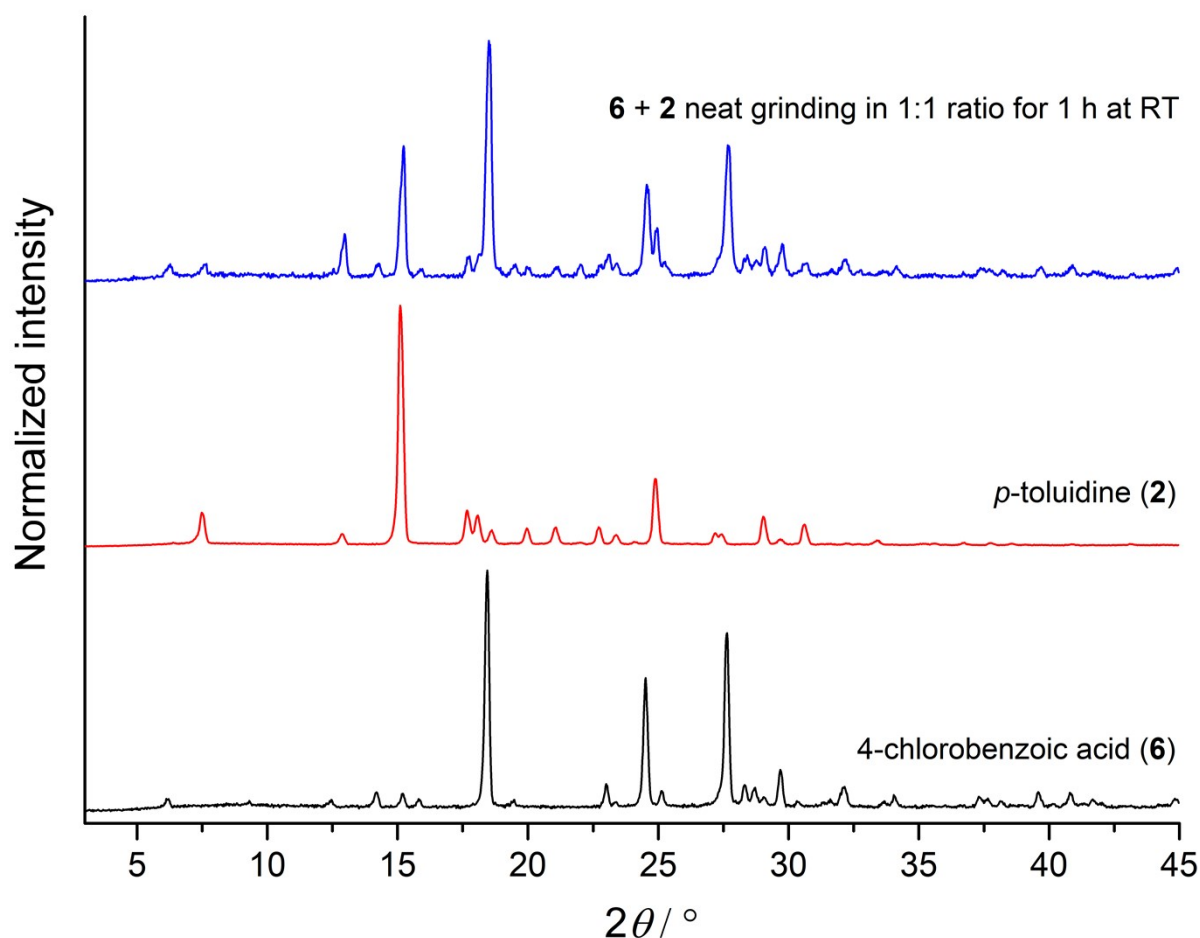
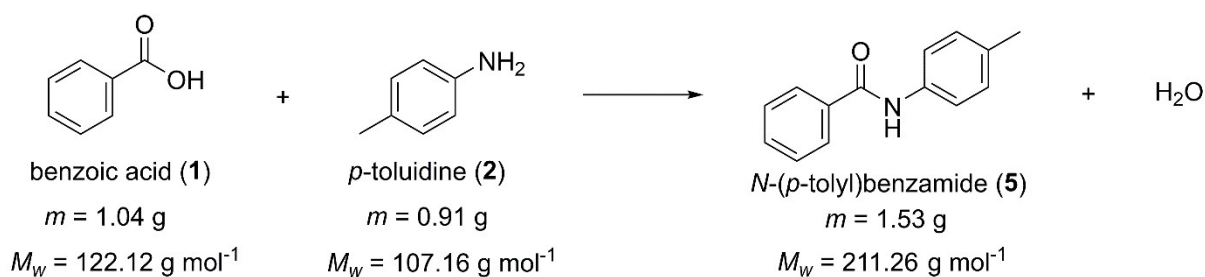


Figure S18. PXRD patterns of the reaction mixture after neat grinding **6** and **2** in 1:1 ratio for 1 h at room temperature and comparison to starting reagents ($\lambda = 1.54 \text{ \AA}$). This resulted in a physical mixture without the salt formation.

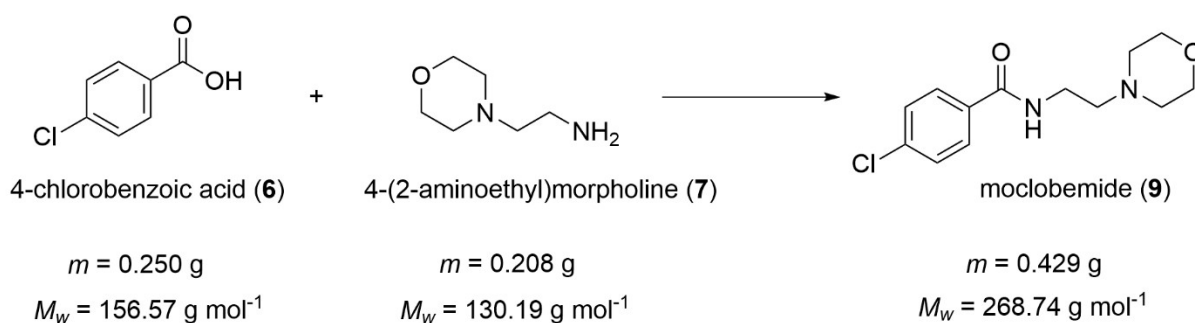
Green chemistry metrics



$$\text{Atom economy (AE)} = 211.26 / (122.12 + 107.16) = 0.921 \text{ or } 92.1\%$$

$$\text{Environmental factor (E-factor)} = (1.04 \text{ g} + 0.91 \text{ g} - 1.53 \text{ g}) / 1.53 \text{ g} = 0.27 \text{ (without purification)}$$

Figure S19. Calculation of green chemistry metric for the synthesis of **5**.



$$\text{Atom economy (AE)} = 268.74 / (156.57 + 130.19) = 0.937 \text{ or } 93.7\%$$

$$\text{Environmental factor (E-factor)} = (0.250 \text{ g} + 0.208 \text{ g} - 0.429 \text{ g}) / 0.429 \text{ g} = 0.07$$

Figure S20. Calculation of green chemistry metric for the synthesis of **9**.

Please note that formation of moclobemide (**9**) from **7** and methyl, ethyl, or benzyl esters of **6** would necessarily lead to a lower atom economy i.e., AE = 89%, 85%, and 71%, respectively, due to the release of alcohols as byproducts instead of water. Moreover, employing esters as activated substrates for mechanochemical amide bond formation requires their use in excess together with almost stoichiometric amounts of additives such as KOtBU,⁵ which undoubtedly increases waste production. On the other hand, using 4-chlorobenzoyl chloride as an activated version of acid **6** also leads to poorer green chemistry metrics (AE = 88%), which is worsened by the need to use additional bases (e.g., pyridine, NH₃, etc.) to neutralize the HCl generated.^{6,7} Finally, mechanochemical formation of moclobemide (**9**) directly from acid **6** and amine **7** requires the use of coupling agents such as CDI, EDC·HCl, or COMU in stoichiometric quantities along with bases, small amounts of solvents, and additives,⁸ thus rendering the process more expensive and lowering its sustainability.

Oven heating

To decouple the thermal and mechanical effects on the amide bond formation, we performed the following two experiments:

- 1) A gently pre-milled 2:1 mixture of benzoic acid and *p*-toluidine was placed in the SS jar (the identical one we used for thermo-milling reactions), closed, and placed in an oven at 190 °C for 1 h. This resulted in 41% conversion to amide **5** (compared to 52% after thermo-milling of the same reaction mixture at 190 °C for 1 h: Table 1, Entry 8 in the manuscript).

- 2) Cocrystal salt **4**, obtained by neat grinding of **1** and **2** in the SS jar (identical one we used for thermo-milling reactions) was placed in an oven at 190 °C for 1 h. This resulted in 48% conversion to amide **5**.

These two experiments demonstrated that heating alone induces amide bond formation, albeit with a lower conversion rate. Starting heating using the intermediate cocrystal salt **4** also has a positive effect on the amide bond formation compared to when starting heating using the pristine reactants. The role of mechanical grinding could be associated with effective mixing, which facilitates mass transfer and results in higher conversion rates. It is also important to note that thermo-milling is more energy efficient than oven heating or magnetic stirring at the same temperature.⁴ Hence, the thermo-mechanochemical approach yields higher conversion rates with a lower energy consumption.

Synthetic procedures

N-(*p*-tolyl)benzamide (**5**)

N-(*p*-tolyl)benzamide (**5**) was prepared by milling 8.5 mmol (1.0 g) of benzoic acid (**1**) and 8.5 mmol (0.9 g) of *p*-toluidine (**2**) were milled for 1 h at 190 °C, after which the hot milling jar was opened and the reaction mixture was allowed to cool to room temperature. Then, the jar was closed and the reaction mixture was milled for additional 2 h at 190 °C. Analysis by ¹H NMR spectroscopy showed the 92% conversion to **5** (Figure S6). The content of the jar was collected and the crude reaction mixture was purified using column chromatography (Al₂O₃) (using a gradient of 100% hexane to 50% ethyl acetate/50% hexane) and recrystallised in EtOH. **5** was obtained as a white solid (1.53 g, 85% yield).

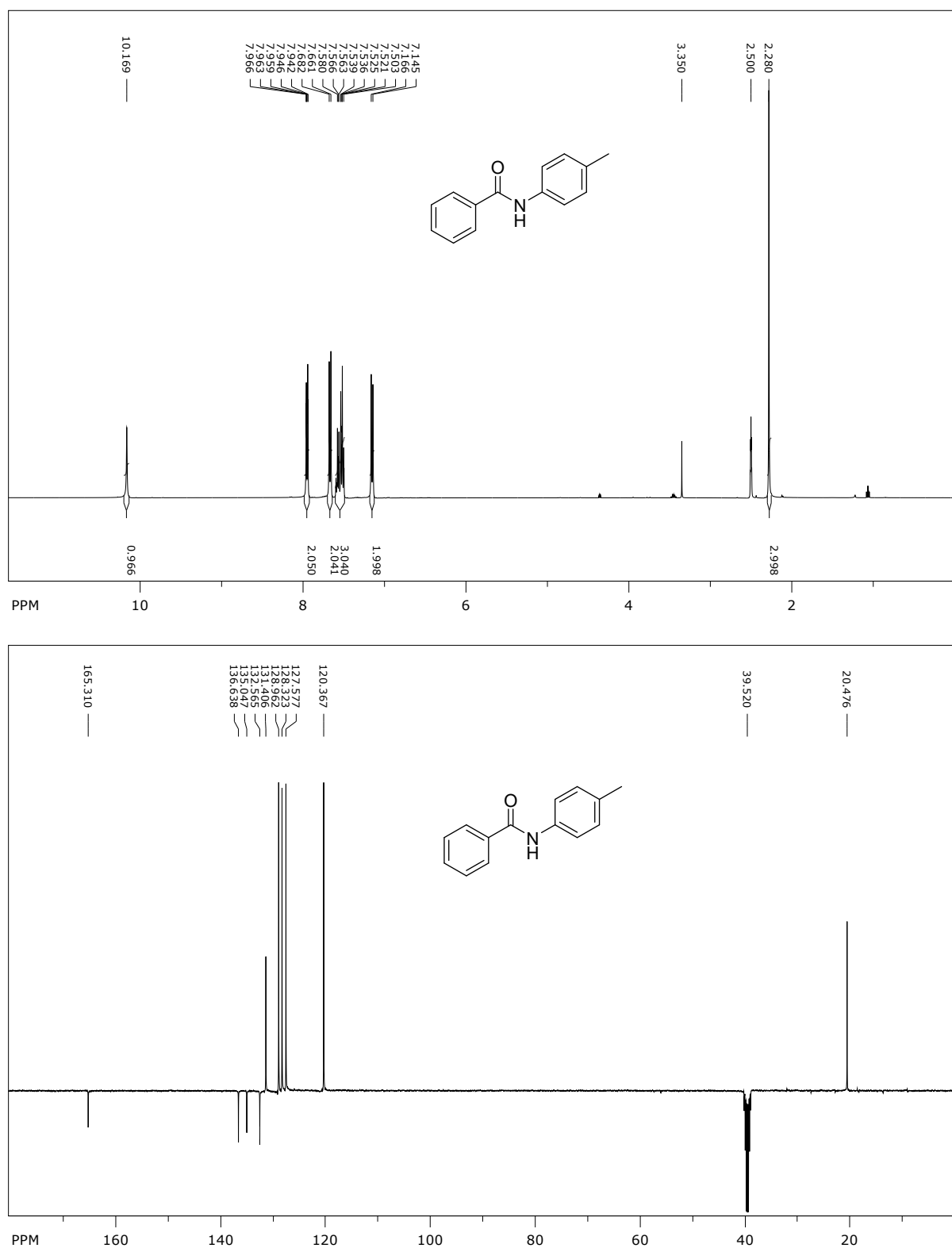


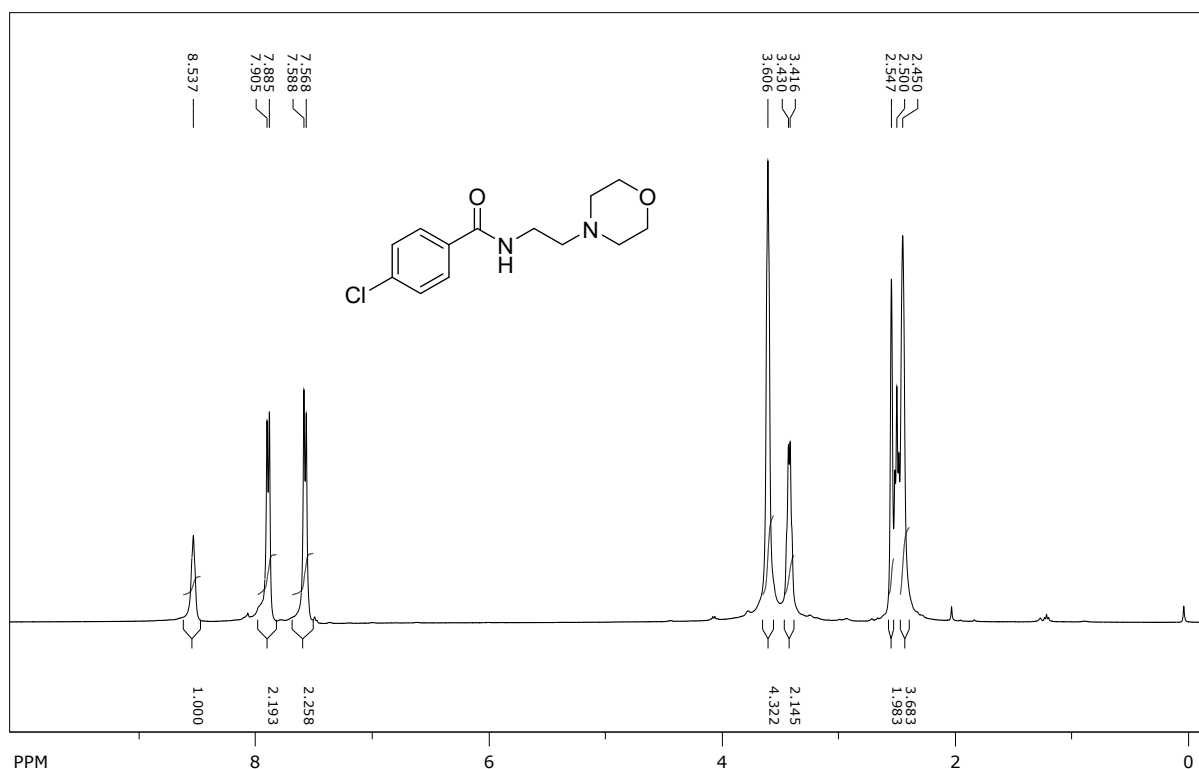
Figure S21. ^1H (400 MHz, $\text{DMSO-}d_6$) and ^{13}C NMR (100 MHz, $\text{DMSO-}d_6$) spectra of *N*-(*p*-tolyl)benzamide (**5**).

^1H NMR for **5** ($\text{DMSO-}d_6$, 400 MHz), δ /ppm: 10.17 (s, 1H), 7.98-7.92 (m, 2H), 7.67 (d, J = 8.3 Hz, 2H), 7.61-7.49 (m, 3H), 7.15 (d, J = 8.3 Hz, 2H), 2.28 (s, 3H). ^{13}C NMR for **5** ($\text{DMSO-}d_6$, 100

MHz), δ /ppm: 165.3 (C=O), 136.6 (C), 135.0 (C), 132.6 (C), 131.4 (CH), 128.9 (CH, 2C), 128.3 (CH, 2C), 127.6 (CH, 2C), 120.4 (CH, 2C), 20.5 (CH₃).

Moclobemide (9)

Moclobemide (**9**) was prepared by milling 1.6 mmol of **6** (0.250 g) and 1.6 mmol of **7** (0.208 g) for 1 h at 190 °C followed by cooling to room temperature and an additional milling for 1 h at 190 °C. That resulted in a quantitative conversion to moclobemide **9** which was isolated pure directly from the milling jar (0.429 g, >99% yield).



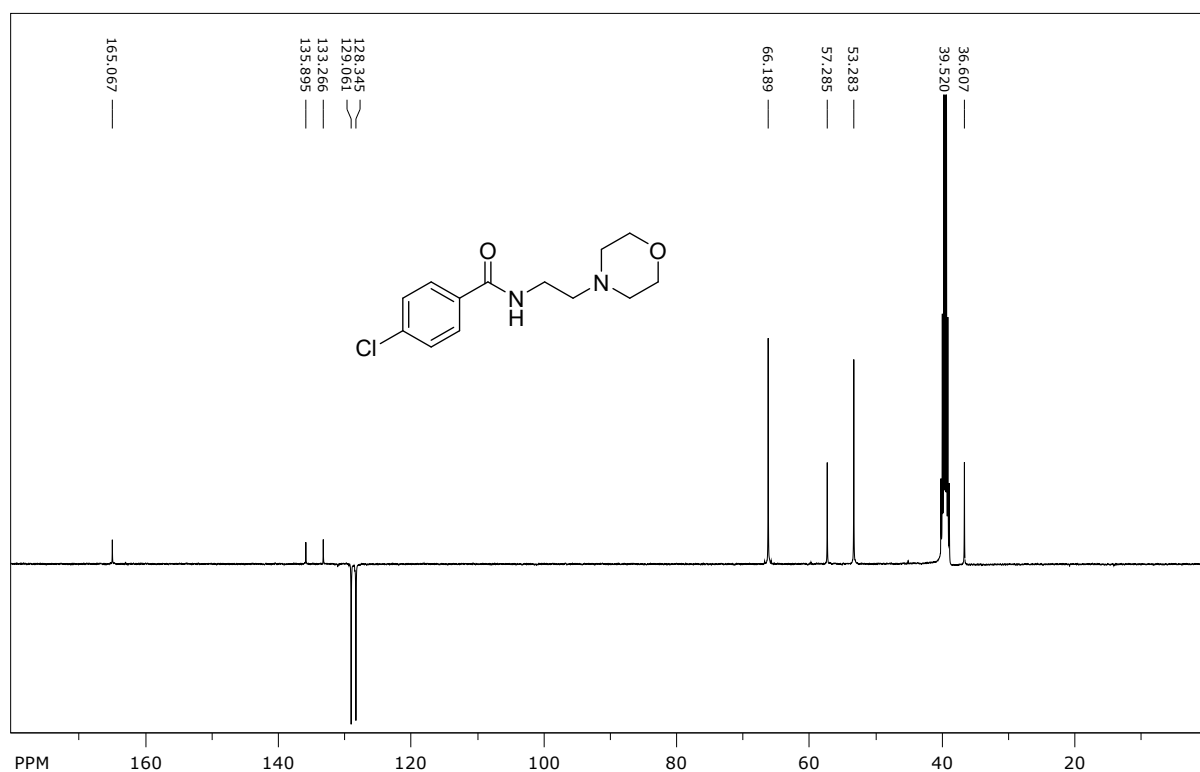
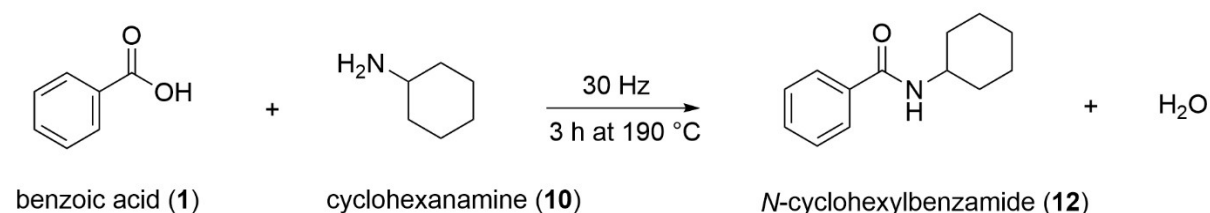


Figure S22. ^1H (400 MHz, $\text{DMSO-}d_6$) and ^{13}C NMR (100 MHz, $\text{DMSO-}d_6$) spectra of moclobemide (**9**).

^1H NMR for **9** ($\text{DMSO-}d_6$, 400 MHz), δ/ppm : 8.54 (br s, 1H), 7.90 (d, $J = 8.1$ Hz, 2H), 7.58 (d, $J = 8.1$ Hz, 2H), 3.61 (br s, 4H), 3.47-3.38 (m, 2H), 2.55 (br s, 2H), 2.45 (br s, 4H). **^{13}C NMR** for **9** ($\text{DMSO-}d_6$, 100 MHz), δ/ppm : 165.1 (C=O), 135.9 (C), 133.3 (C), 129.1 (CH, 2C), 128.3 (CH, 2C), 66.2 (CH_2 , 2C), 57.3 (CH_2), 53.3 (CH_2 , 2C), 36.6 (CH_2).

N-cyclohexylbenzamide (**12**)



N-cyclohexylbenzamide (**12**) was prepared by milling 1.0 mmol of **1** (0.122 g) and 1.0 mmol of cyclohexanamine **10** (0.115 mL) for 1 h at 190 °C followed by cooling to room temperature and an additional milling for 2 h at 190 °C. The content of the jar was collected, suspended in EtOAc (20 mL), filtered through a silica plug, washed with a saturated solution of NaHCO_3 (3 x 7 mL) and dried over anhydrous Na_2SO_4 . **12** was obtained as an off white solid (0.072 g, 35% yield).

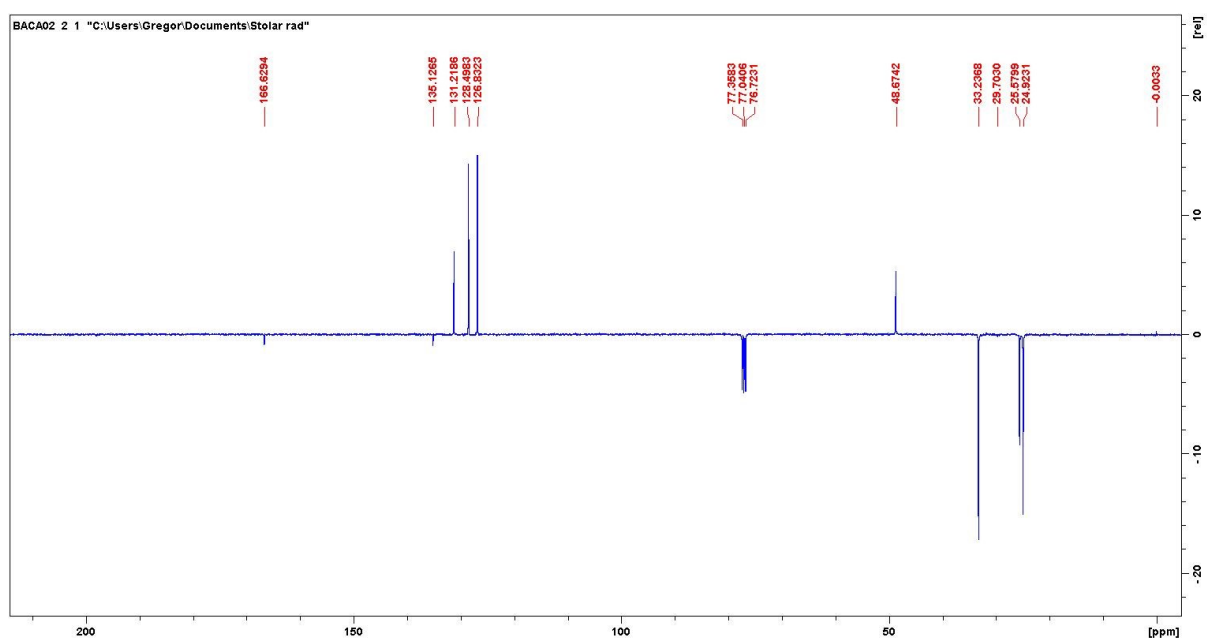
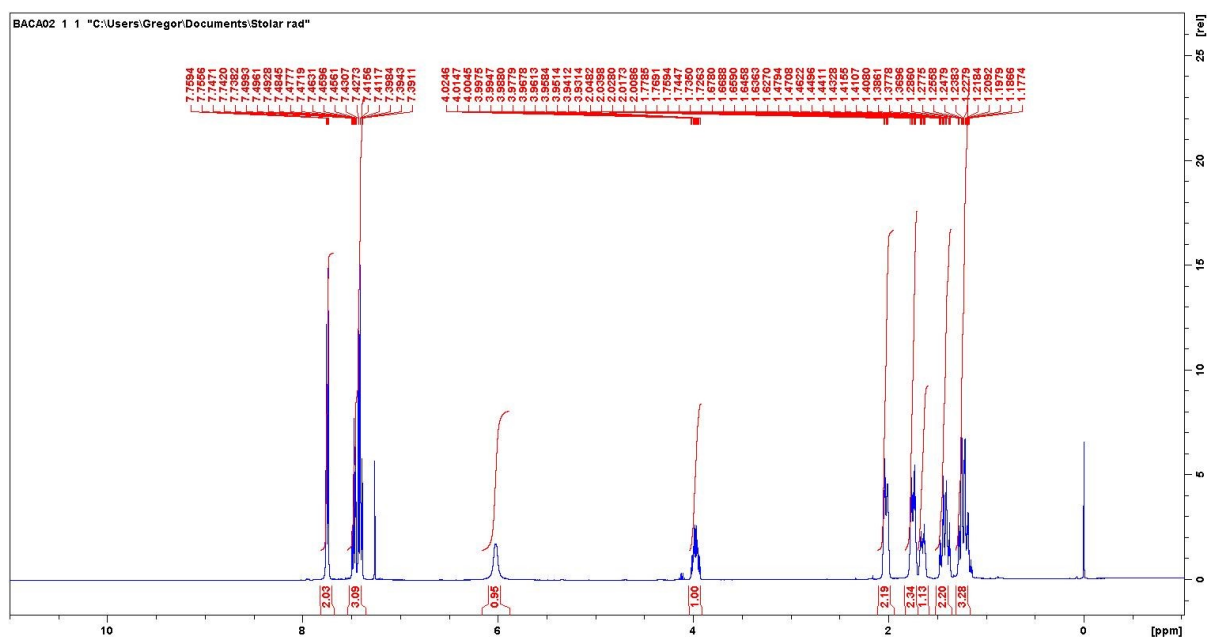
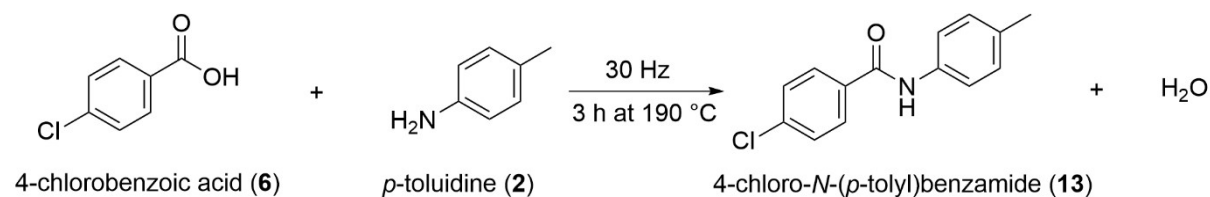


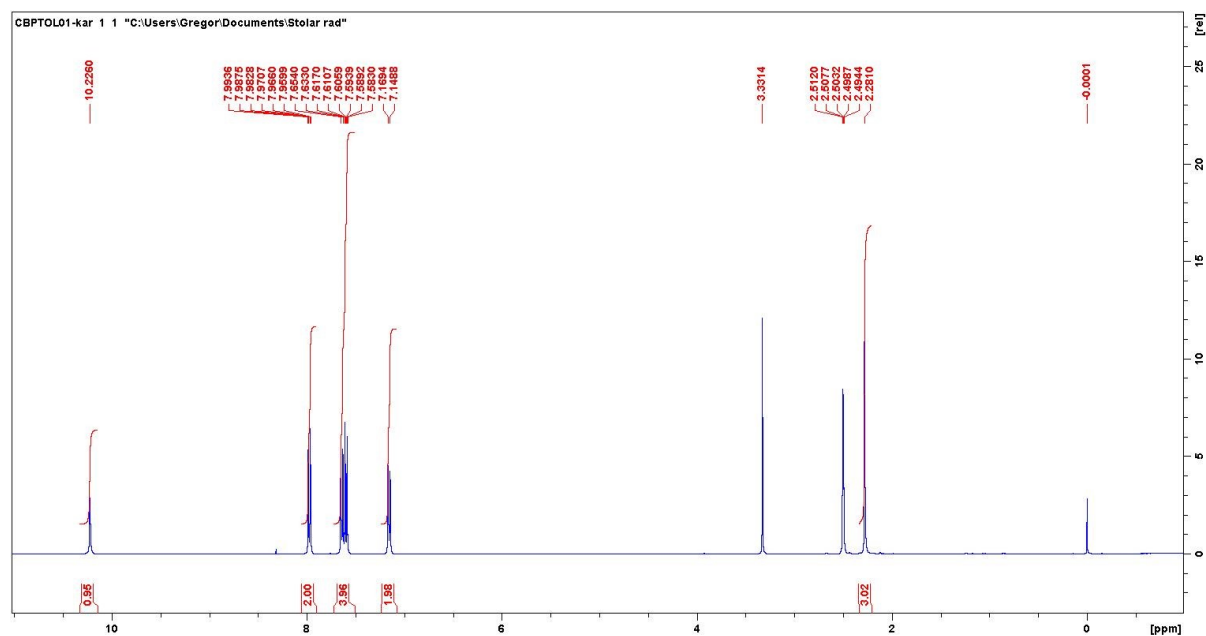
Figure S23. ^1H (400 MHz, CDCl_3) and ^{13}C NMR (100 MHz, CDCl_3) spectra of *N*-cyclohexylbenzamide (**12**).

^1H NMR for **12** (CDCl_3 , 400 MHz), δ/ppm : 7.77-7.73 (m, 2H), 7.51-7.38 (m, 3H), 6.03 (br s, 1H), 4.04-3.92 (m, 1H), 2.08-1.98 (m, 2H), 1.81-1.71 (m, 2H), 1.70-1.61 (m, 1H), 1.49-1.36 (m, 2H), 1.30-1.17 (m, 3H). ^{13}C NMR for **12** (CDCl_3 , 100 MHz), δ/ppm : 166.6 (C=O), 135.1 (C), 131.2 (CH), 128.5 (CH), 126.8 (CH), 48.7 (CH), 33.2 (CH_2 , 2C), 25.6 (CH_2), 24.9 (CH_2 , 2C).

4-chloro-*N*-(*p*-tolyl)benzamide (**13**)



4-chloro-*N*-(*p*-tolyl)benzamide (**13**) was prepared by milling 1.0 mmol of **6** (0.157 g) and 1.0 mmol of **2** (0.107 g) for 1 h at 190 °C followed by cooling to room temperature and an additional milling for 2 h at 190 °C. The content of the jar was collected, suspended in EtOAc (20 mL), filtered through a silica plug, washed with a saturated solution of NaHCO₃ (3 x 7 mL), 0.1 M HCl (3 x 7 mL) and brine (5 mL) and dried over anhydrous Na₂SO₄. **13** was obtained as an off white solid (0.086 g, 35% yield).



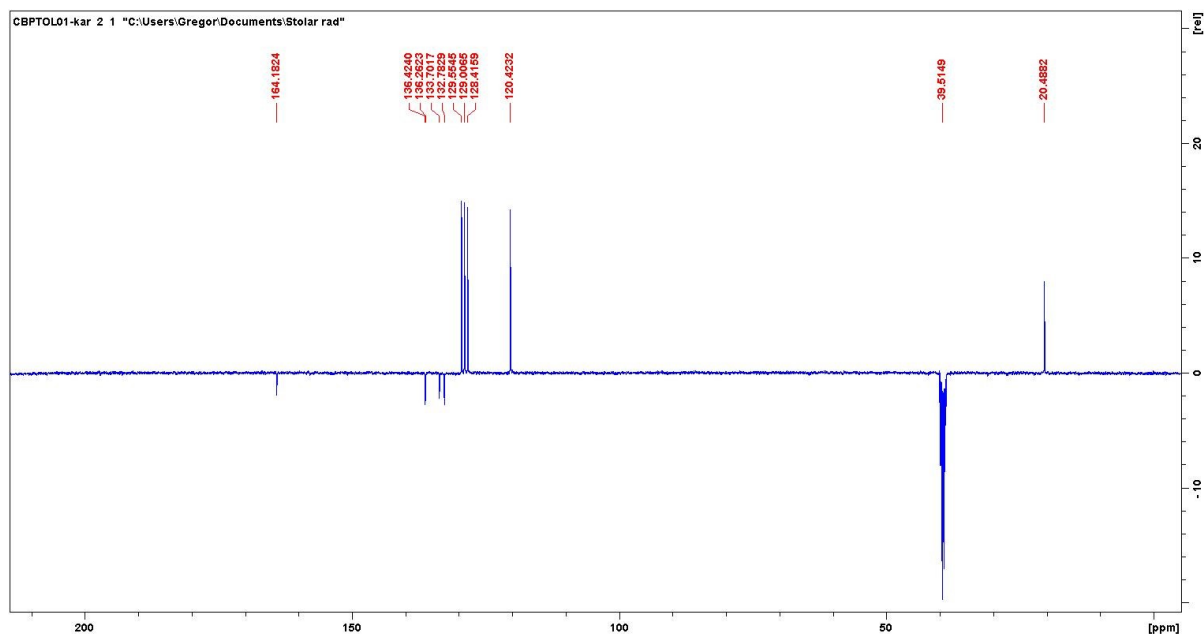


Figure S24. ^1H (400 MHz, $\text{DMSO-}d_6$) and ^{13}C NMR (100 MHz, $\text{DMSO-}d_6$) spectra of 4-chloro-*N*-(*p*-tolyl)benzamide (**13**).

^1H NMR for **13** ($\text{DMSO-}d_6$, 400 MHz), δ/ppm : 10.23 (s, 1H), 7.98 (d, $J = 8.6$ Hz, 2H), 7.64 (d, $J = 8.3$ Hz, 2H), 7.0 (d, $J = 8.6$ Hz, 2H), 7.16 (d, $J = 8.3$ Hz, 2H), 2.28 (s, 3H). ^{13}C NMR for **13** ($\text{DMSO-}d_6$, 100 MHz), δ/ppm : 164.2 (C=O), 136.4 (C), 136.3 (C), 133.7 (C), 132.8 (CH), 129.6 (CH, 2C), 129.0 (CH, 2C), 128.4 (CH, 2C), 120.4 (CH, 2C), 20.5 (CH_3).

References

1. CrysAlisPro, Rigaku Oxford Diffraction, 2018, version: 1.171.39.46, Rigaku Corporation, Oxford, UK.
2. G. M. Sheldrick, *Acta Cryst.* 2015, **A71**, 3–8.
3. A. L. Spek, *Acta Crystallogr. D*, 2009, **D65**, 148–155.
4. J. Alić, T. Stolar, Z. Štefanić, K. Užarević and M. Šekutor, *ACS Sustainable Chem. Eng.* 2023, **11**, 617–624.
5. W. I. Nicholson, F. Barreteau, J. A. Leitch, R. Payne, I. Priestley, E. Godineau, C. Battilocchio and D. L. Browne, *Angew. Chem., Int. Ed.*, 2021, **60**, 21868–21874.
6. J. D. More, *J. Chem. Edu.*, 2008, **85**, 1424–1425.
7. W. Burkhard and P.-C. Wyss, Morpholino Containing Benzamides. U.S. Patent 4, 210, 754, July 1, 1980.
8. M. Lavayssiere and F. Lamaty, *Chem. Commun.*, 2023, **59**, 3439–3442.